

# Preparation and Properties of Multiwalled Carbon Nanotube/Polycaprolactone Nanocomposites

Khalid Saeed, Soo-Young Park

Department of Polymer Science, Kyungpook National University, Daegu 702-701, Republic of Korea

Received 28 September 2006; accepted 21 November 2006

DOI 10.1002/app.25902

Published online in Wiley InterScience (www.interscience.wiley.com).

**ABSTRACT:** Multiwalled carbon nanotube/polycaprolactone nanocomposites (MWNT/PCL) were prepared by *in situ* polymerization, whereby as-received MWNTs (P-MWNTs) and purified MWNTs (A-MWNTs) were used as reinforcing materials. The A-MWNTs were purified by nitric acid treatment, which introduced the carboxyl groups (COOH) on the MWNT. The micrographs of the fractured surfaces of the nanocomposites showed that the A-MWNTs in A-MWNT/PCL were better dispersed than P-MWNTs in PCL matrix (P-MWNT/PCL). Percolation thresholds of the P-MWNT/PCL and A-MWNT/PCL, which were studied by rheological properties, were found at  $\sim 2$  wt % of the MWNT. The conductivity of the P-MWNT/PCL was between  $10^{-1}$  and  $10^{-2}$  S/cm by loading of 2 wt % of

MWNT although that of the A-MWNT/PCL reached  $\sim 10^{-2}$  S/cm by loading of 7 wt % of MWNT. The conductivity of the P-MWNT/PCL was higher than that of the A-MWNT/PCL at the entire range of the studied MWNT loading, which might be due to the destruction of  $\pi$ -network of the MWNT by acid treatment, although the A-MWNT/PCL was better dispersed than the P-MWNT/PCL. The amount of the MWNT at which the conductivity of the nanocomposite started to increase was strongly correlated with the percolation threshold. © 2007 Wiley Periodicals, Inc. *J Appl Polym Sci* 104: 1957–1963, 2007

**Key words:** polycaprolactone; *in situ* polymerization; multiwalled carbon nanotubes; composites; electrical properties

## INTRODUCTION

Carbon nanotubes (CNTs) display a wide range of unique mechanical, optical, and electrical properties along with chemical stability.<sup>1–3</sup> The CNTs can be described as a graphene sheet rolled into a tube, which can alter either metallic or semiconducting properties depending upon their chirality and diameter, thus making them an ideal reinforcing filler in composite materials. Because of the unique properties of CNTs, researchers have paid great attention to utilize these remarkable characteristics for engineering applications such as polymeric composites, hydrogen storage,<sup>4</sup> actuators,<sup>5</sup> field-emission materials,<sup>6</sup> chemical sensors,<sup>7</sup> and nanoelectronic devices.<sup>8</sup>

The inferior properties of polymers such as their electrical conductivity, mechanical properties, and thermal conductivity can be enhanced by incorporation of even a minute amount of CNTs. In CNT/polymer composites, the CNTs cannot be dispersed by simple mixing. This is because they are present in the form of bundles and ropes through a van der Waals attraction among the tubes in combination with their high surface area. In addition, polymeric materials,

whose viscosities are relatively higher than low molar mass materials, have difficulty in penetrating the CNT bundles. As an alternative to simple mixing, chemical functionalization on the CNT wall was used, which not only disperses CNTs in an organic solvent,<sup>9</sup> water,<sup>10,11</sup> or polymer matrix,<sup>12</sup> but also attaches chemically with polymeric materials.<sup>13</sup> Functional groups can be introduced either on the sidewall by fluorination, arylation, nitrene cycloaddition, 1,3-dicycloaddition,<sup>14,15</sup> Friedel-Crafts acylation,<sup>16,17</sup> or at the end of CNTs by acid treatment.<sup>18</sup> In sidewall functionalization, the carbon atoms of the CNTs react with the functional groups which are thereby converted from  $sp^2$  to  $sp^3$  and their electronic properties are changed significantly. The end-functionalization does not change the mechanical and electrical properties significantly because it does not destroy the  $\pi$ -network of the CNTs. Noncovalent functionalization is another technique that can be used to modify CNTs, and which does not destroy the conjugation system in the CNTs. A number of routes to the noncovalent modification of CNTs have been reported such as polymer wrapping,<sup>19</sup> the adsorption of amine,<sup>20</sup> and radiofrequency glow-discharge plasma modification.<sup>21</sup>

Polycaprolactone (PCL) is a linear aliphatic polyester, which is known for its unique biocompatibility, degradability,<sup>22</sup> and is used in degradable packing and drug delivery systems in medical supplies.

Correspondence to: S.-Y. Park (psy@knu.ac.kr).

Although PCL is compatible with a wide range of polymers, its low melting point has been a disadvantage in many applications. To expand its applicability, the blending of PCL with polymer<sup>23</sup> or nanomaterials can be incorporated during PCL polymerization.<sup>24</sup> Recently, we purified multiwalled CNTs (MWNTs) by nitric acid and used it as a reinforcing material in PCL. The nanocomposites were prepared with the as-received MWNTs and purified MWNTs, and their structures and properties were compared to determine the relationship between the dispersion and other properties such as conductivity and mechanical properties.

## EXPERIMENTAL

### Materials

$\epsilon$ -Caprolactone (99% purity) and stannous octoate (95% purity) were purchased from Aldrich<sup>®</sup> and Sigma<sup>®</sup>, respectively, and used as received. Nitric acid (64–66% purity) was purchased from a local company, Ducksan. The MWNTs (CVD MWNT 95) were supplied by Iljin Nanotech<sup>®</sup> and manufactured by thermal chemical vapor deposition.<sup>25</sup> Diameter and length of the CVD MWNT 95 were 10–20 nm and 10–50  $\mu\text{m}$ , respectively, and its purity was higher than 97 wt %.

### Purification of MWNTs

The MWNT was purified by an acid treatment of MWNT (A-MWNT), whereby 3 g of MWNTs were sonicated in 300 mL of 5M  $\text{HNO}_3$  for 2 h and then refluxed at 120°C for 12 h. The A-MWNTs were separated from  $\text{HNO}_3$  by filtration and then washed with distilled water until they were free from acid. The A-MWNTs were dried in a vacuum oven and stored for further use. The carboxyl groups were also introduced on MWNT during purification with  $\text{HNO}_3$ .<sup>14</sup>

Scheme 1 shows the *in situ* polymerization of P-MWNT/PCL and A-MWNT/PCL nanocomposites. The procedure for synthesizing P-MWNT/PCL is as follows: A predetermined percentage of P-MWNT

and 20 mL of  $\epsilon$ -caprolactone were introduced in a three-neck round bottom flask. The mixture was sonicated at room temperature for 3 h to produce a homogenous dispersion of P-MWNTs in  $\epsilon$ -caprolactone, then 0.03 mL of stannous octoate [ $\text{Sn}(\text{Oct})_2$ ] were added to the suspension. The flask was then transferred to a preheated oil bath (170°C) and heated for 4 h by mechanical stirring, under a nitrogen atmosphere. The same procedure was adopted for the A-MWNT/PCL nanocomposites.

## Characterization

### Thermal properties

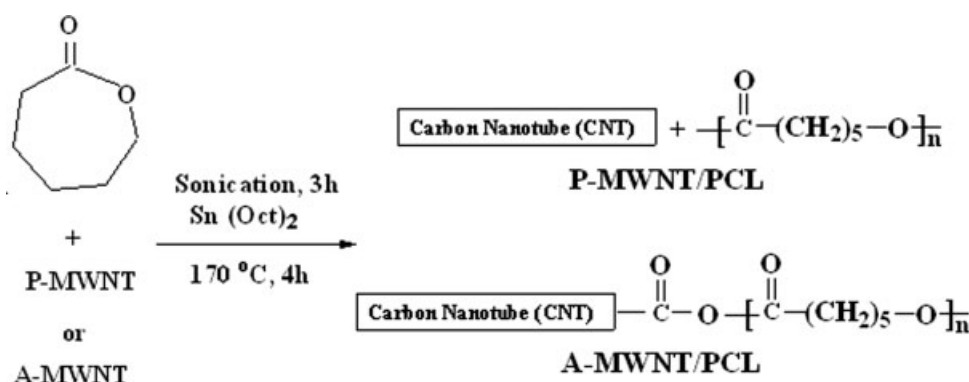
The thermal properties of the PCL and the composites were studied by DSC and TGA. The DSC analyses were carried out on a Dupont 2000 Thermal Analyzer. A specific amount of sample was sealed in aluminum sample pans and prepared by compression molding. DSC thermograms were obtained at heating and cooling rates of 10°C/min under a nitrogen atmosphere to diminish oxidation. The TGA of PCL and the composites were obtained in a nitrogen atmosphere, at a heating rate of 20°C/min from room temperature to 900°C using a -TA4000/Auto DSC 2910 System.

### Polarized optical microscopy

Polarized optical microscopic photographs were obtained using a Moram JI-213 Polarized Optical Microscope. The sample was melted on a heater and squeezed between two glass slides at 100°C for 10 min, quickly transferred to hot stage, and annealed at 50°C for 3 h.

### Dynamic mechanical analysis

DMA analysis was performed on the samples 20(length)  $\times$  5(width)  $\times$  0.17(thickness)  $\text{mm}^3$  by using Parkin-Elmer, a Diamond Dynamic Mechanical Analyzer, in a temperature range between –100 and 60°C, at a frequency of 1 Hz, and a heating rate of 5°C/min.



**Scheme 1** *In situ* polymerization of P-MWNT/PCL and A-MWNT/PCL nanocomposites.

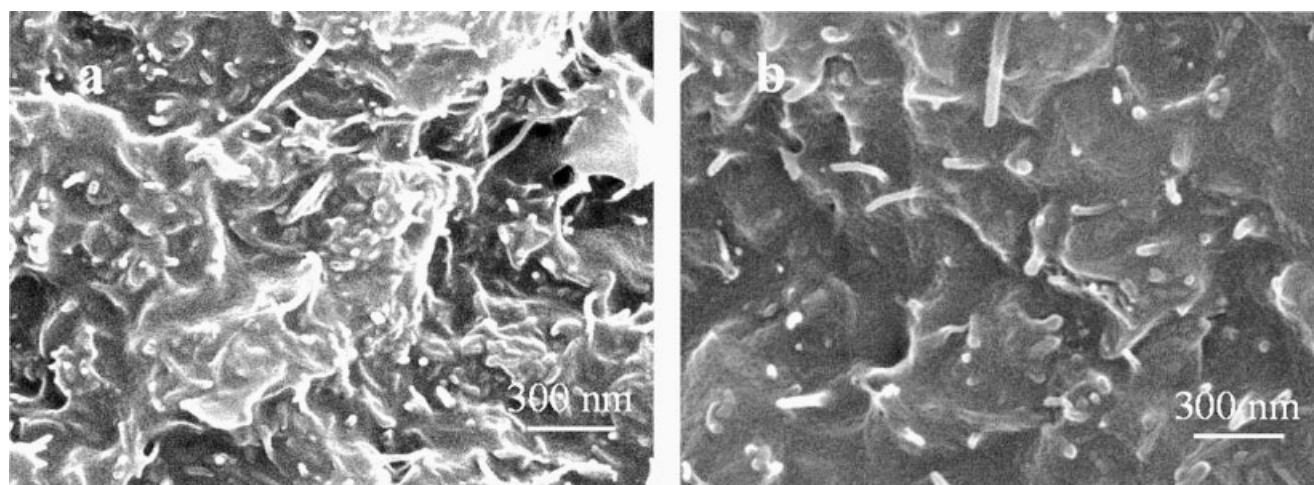


**Figure 1** SEM images of the fractured surface (a) P-MWNT (5 wt %)/PCL and (b) A-MWNT (5 wt %)/PCL.

#### Rheometer measurements

Rheometer measurements were performed on a Physica, UDS 200 Rheometer. All samples (thickness of 0.3 mm) were measured at 80°C in an angular frequency range between 0.1 and 100 rad/s and the strain was 5%.

#### Electrical conductivity measurements

The conductivity of the MWNT/PCL nanocomposites was measured at ambient temperature with (Ecopia, HMS-3000) four-point probe method. The

dimensions of the samples were about 15(length)  $\times$  15(width)  $\times$  0.15(thickness) mm<sup>3</sup> and their ends were coated with a platinum paste to ensure good electrical contact. The electrical conductivity limit of the instrument is in the range of 10<sup>3</sup>–10<sup>−6</sup> S/cm.

## RESULTS AND DISCUSSION

Figure 1 shows the SEM microphotographs of the fractured surfaces of the P-MWNT (5 wt %)/PCL and A-MWNT (5 wt %)/PCL, which indicate that A-MWNT dispersed more as compared with MWNT. The dispersion of MWNT in A-MWNT/PCL is due

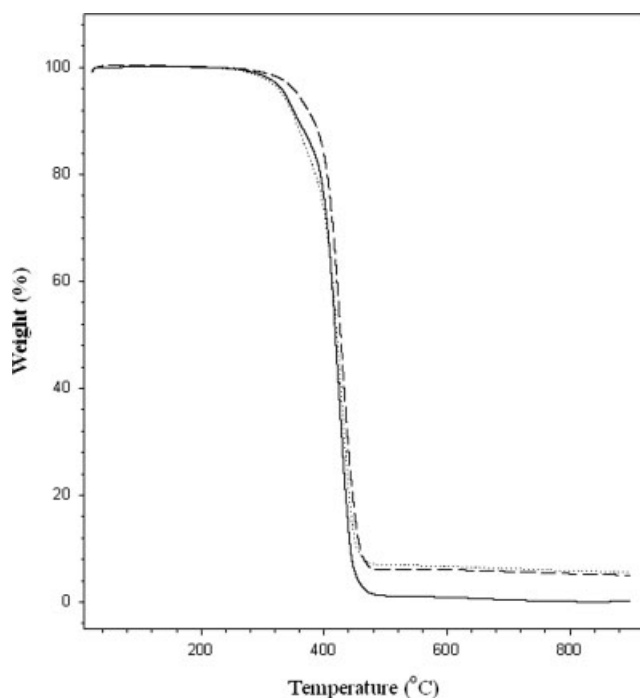


**Figure 2** TGA thermograms of PCL (—), P-MWNT (5 wt %)/PCL (···), and A-MWNT (5 wt %)/PCL (---).

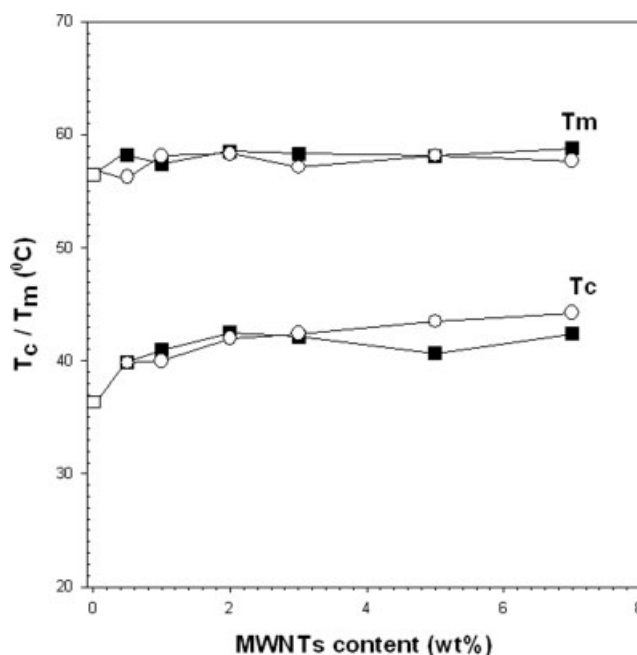


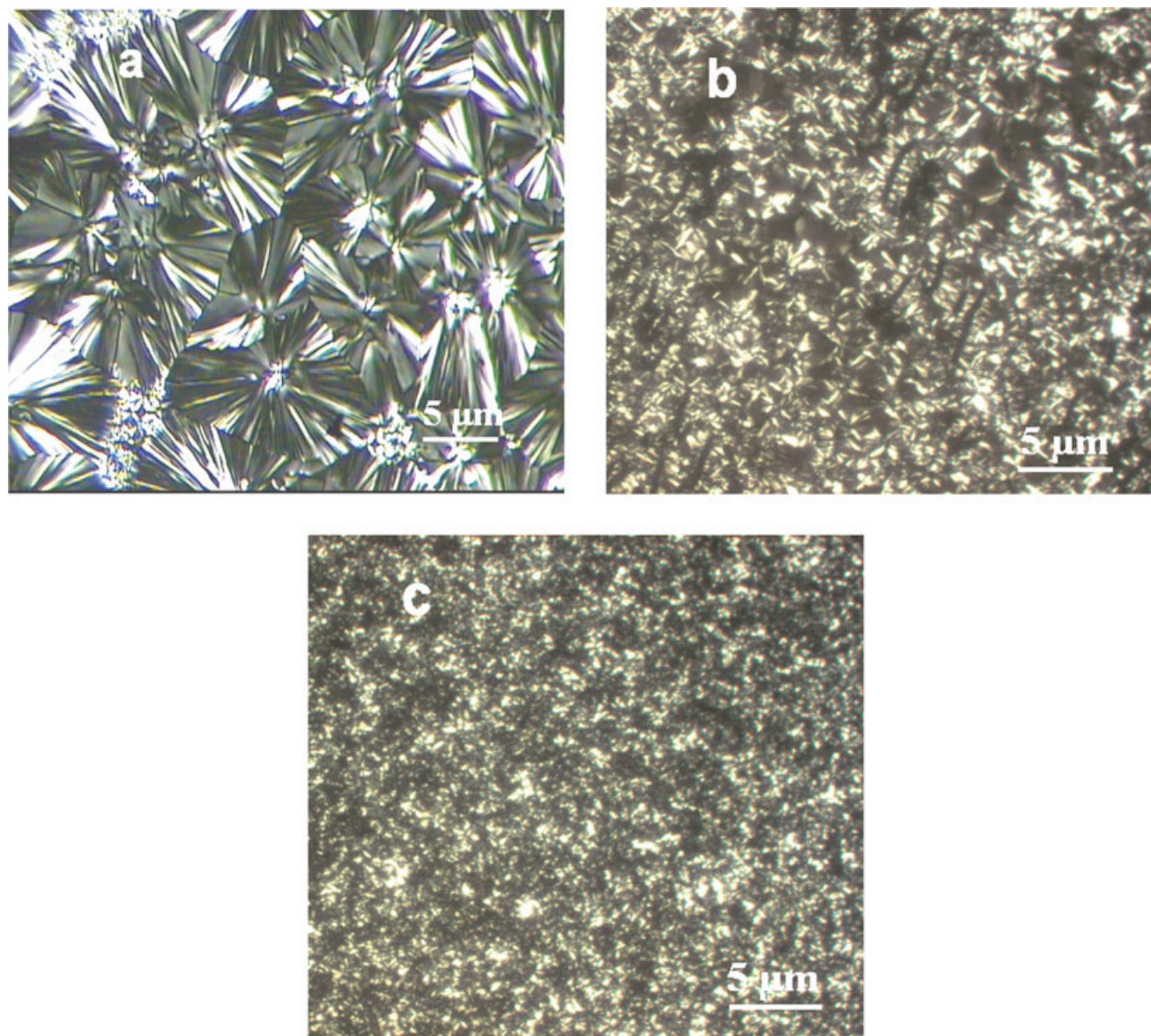
**Figure 3** Melting and crystallization temperatures of (□) PCL, (■) P-MWNT/PCL, and (○) A-MWNT/PCL, as a function of the amounts of MWNT.

to the chemical modification of the MWNT during purification, which causes more compatibility with PCL.<sup>9,10</sup>

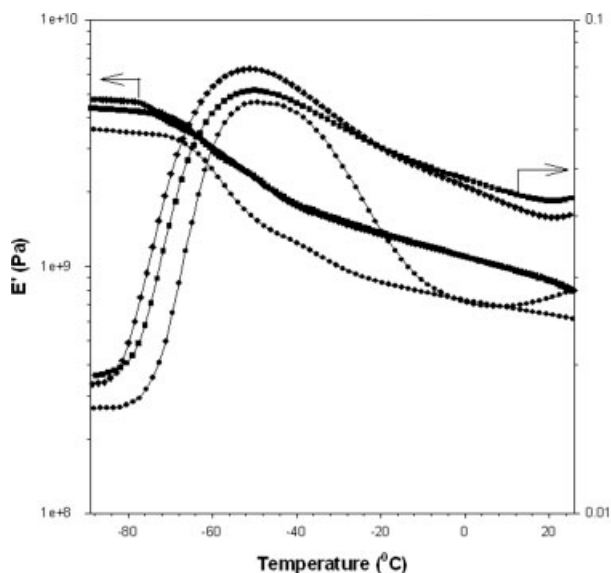
Figure 2 shows TGA curves of the PCL, P-MWNT (5 wt %)/PCL, and A-MWNT (5 wt %)/PCL. The pure PCL and P-MWNT/PCL started to lose weight at 310°C and completely decomposed at 460°C. The A-MWNT/PCL started to lose weight at about 330°C, which is 20°C higher than the pure PCL and P-MWNT/PCL. The increase of the degradation temperature indicates that the incorporation of A-MWNT into the PCL exerts a thermal stabilizing effect in the composite.

Figure 3 shows the changes in the melting and crystallization (crystallization from the melt state

upon cooling) temperatures of PCL, P-MWNT/PCL, and A-MWNT/PCL as a function of the amount of MWNTs. The melting and crystallization temperatures of the PCL were 57 and 36°C, respectively. The melting temperatures of all nanocomposites were in a narrow range between 57 and 59°C. The crystallization temperatures of P-MWNT/PCL and A-MWNT/PCL slightly increased from that of PCL with the addition of MWNT. The temperatures leveled off at 43°C by adding 2 wt % MWNT. The MWNTs in P-MWNT/PCL and A-MWNT/PCL could be acted as nucleation agents for PCL crystallization<sup>26,27</sup> and caused the crystallization rate to increase (the crystal was produced earlier during cooling) when compared with the neat PCL.



**Figure 4** Polarized optical micrographs of (a) PCL, (b) A-MWNT (5 wt %)/PCL, and (c) P-MWNT (5 wt %)/PCL, which were prepared by cooling from a melt state and annealed at 50°C for 3 h period under cross polarizing filters. [Color figure can be viewed in the online issue, which is available at [www.interscience.wiley.com](http://www.interscience.wiley.com).]



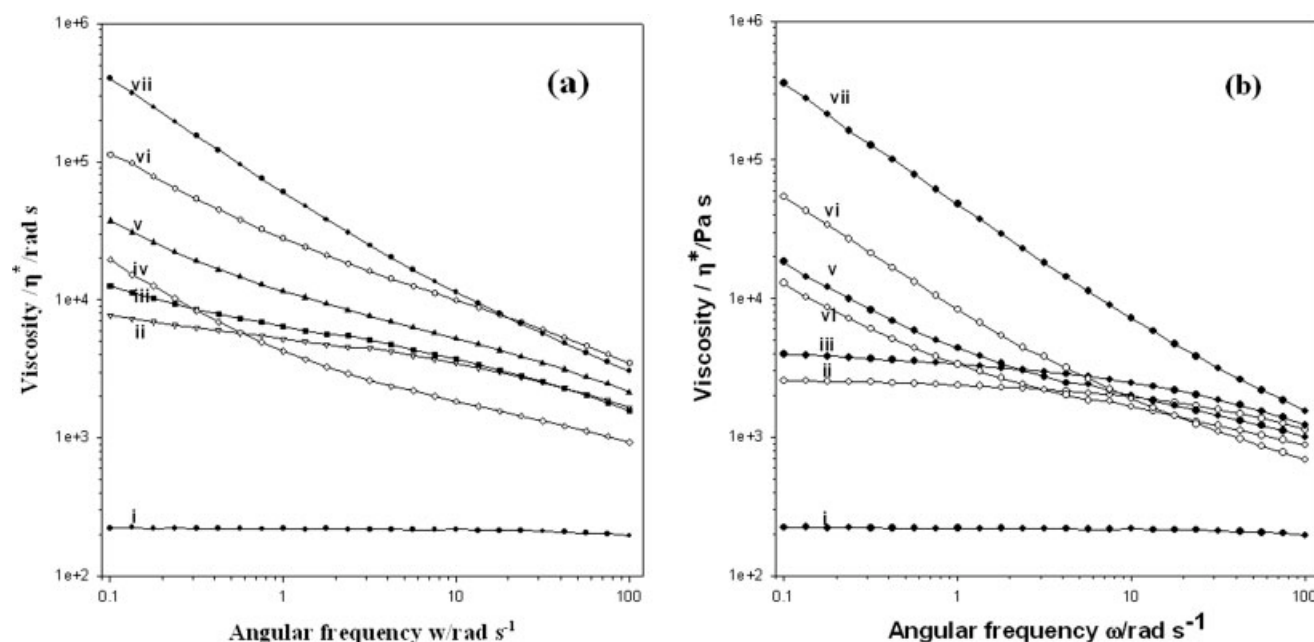
**Figure 5** Storage modulus ( $E'$ ) and  $\tan \delta$  of (●) PCL, (◆) P-MWNTs (3 wt %)/PCL, and (■) A-MWNTs (3 wt %)/PCL.

Figure 4 shows the polarized optical micrographs of PCL, P-MWNT (5 wt %)/PCL, and A-MWNT (5 wt %)/PCL, which were prepared by cooling from the melt state and annealed at 50°C for 3 h period under cross polarizing filters. The polarized optical micrograph of PCL showed a Maltese cross pattern with a size of 13  $\mu\text{m}$  [Fig. 4(a)], while granular crystals were observed for A-MWNT/PCL [Fig. 4(b)] and P-MWNT/PCL [Fig. 4(c)]. The spherulites observed

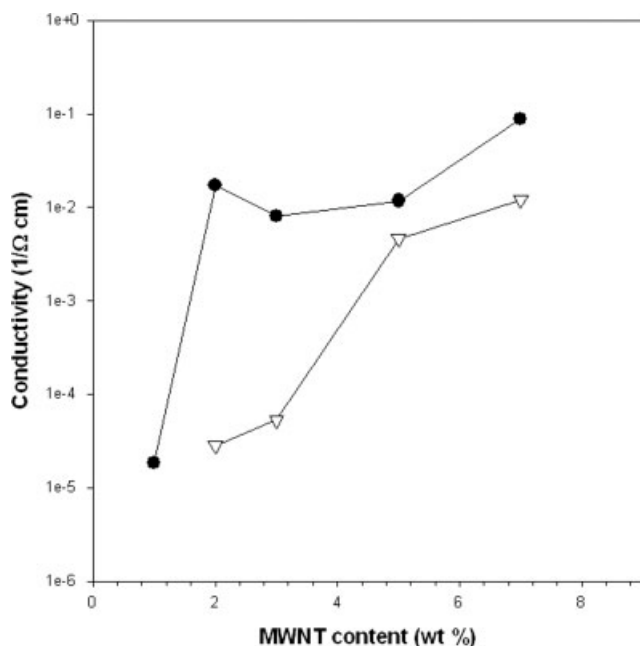
in PCL are similar to the reported pattern,<sup>28</sup> although there were some irregularities present in the spherulites. The nucleation role of MWNT in P-MWNT/PCL and A-MWNT/PCL might cause small granular spherulites.<sup>29</sup>

Figure 5 shows the changes of the storage modulus ( $E'$ ) and  $\tan \delta$  of the PCL, P-MWNT (3 wt %)/PCL, and A-MWNT (3 wt %)/PCL, as a function of temperature. The  $E'$  increased by adding 3 wt % of MWNT for both of MWNT (3 wt %)/PCL and A-MWNT (3 wt %)/PCL as compared with the pure PCL. The temperature at the maximum point in  $\tan \delta$  (representing the glass transition temperature [ $T_g$ ]) did not change significantly, but the peak was broadened in the high temperature region by adding MWNTs in the nanocomposite. It is likely that the major parts of the polymer, which were away from the MWNTs, retained the glass transition temperature, but the segments that were close to the MWNTs, were less mobile and showed an increase in the glass transition temperature. Similar results of MWNT/PMMA have been reported by Jin et al.<sup>30</sup>

Figure 6 shows the complex viscosities ( $\eta^*$ s) of the P-MWNT/PCL and A-MWNT/PCL, as a function of the frequencies with different amounts of MWNTs. The  $\eta^*$ s at low frequencies increased as the MWNT content increased for P-MWNT/PCL and A-MWNT/PCL. The  $\eta^*$ s of P-MWNT/PCL and A-MWNT/PCL showed Newtonian behavior for the MWNT contents less than 2 wt %, although those of higher than 2 wt % showed profound shear-thinning behavior. This viscosity behavior indicates that a percolation



**Figure 6** Complex viscosities ( $\eta^*$ s) of (a) P-MWNTs/PCL and (b) A-MWNTs/PCL; weight of MWNT (i) 0%, (ii) 0.5%, (iii) 1%, (iv) 2%, (v) 3%, (vi) 5%, (vii) 7%.



**Figure 7** Conductivities of the P-MWNT/PCL (●) and A-MWNT/PCL (▽) films as a function of the MWNT amounts.

threshold, which represents a starting MWNT content of a three-dimensional network was 2 wt % for both the P-MWNT/PCL and A-MWNT/PCL.<sup>31–33</sup> We also found similar behaviors for  $\eta'$  and  $\eta''$  with  $\eta^*$ .

Figure 7 shows the conductivities of the P-MWNT/PCL and A-MWNT/PCL, as a function of the MWNT amounts. Both composites showed high electrical conductivity at low filler loading. In agreement with rheological measurements this onset in the conductivity is attributed to a percolation of MWNT in the insulating polymer matrix. The conductivity of the A-MWNT/PCL increased continuously with an increase in the MWNT amounts and reached  $10^{-2}$  S/cm for a 7 wt % MWNT content. The conductivities of the P-MWNT/PCL increased very rapidly and leveled off between  $10^{-1}$  S/cm and  $10^{-2}$  S/cm after 2 wt %. This conductivity ( $10^{-2}$  S/cm) is significantly high for the 2 wt % MWNT content. This high conductivity indicates that the MWNTs were well dispersed in the nanocomposite system. The A-MWNT/PCL shows less conductivity as compared with the MWNT/PCL. It might be due to the acid treatment, which usually opens up the end-capsule of the carbon nanotube and destroys the  $\pi$ -network.

## CONCLUSIONS

We prepared two nanocomposite systems, P-MWNT (as-received one)/PCL and A-MWNT/PCL by using an *in situ* polymerization method, to study the effects of the dispersion and purification of MWNTs

on the thermal, mechanical, and electrical properties of nanocomposites. The A-MWNTs were purified by acid treatment, which also introduced the carboxyl groups on MWNTs. The crystallization temperatures of P-MWNT/PCL and A-MWNT/PCL increased because of nucleation by MWNTs. Granular spherulites were observed for P-MWNT/PCL and A-MWNT/PCL while the typical Maltese-cross spherulites were observed for pure PCL. The P-MWNTs and A-MWNTs were well dispersed in the PCL matrix, as indicated by the low percolation threshold ( $\sim 2$  wt %) in the rheological data. The conductivity of the P-MWNT/PCL was between  $10^{-1}$  to  $10^{-2}$  S/cm by loading of 2 wt % of MWNT although that of the A-MWNT/PCL reached  $\sim 10^{-2}$  S/cm by loading of 7 wt % of MWNT.

This work was supported by Ministry of Commerce, Industry, and Energy.

## References

- Iijima, S. *Nature* 1991, 354, 56.
- Wong, E. W.; Sheehan, P. E.; Lieber, C. M. *Science* 1997, 277, 1971.
- Lillehei, P. T.; Park, C.; Rouse, J. H.; Siochi, E. J. *Nano Lett* 2002, 2, 827.
- Liu, C.; Fan, Y. Y.; Liu, M.; Cong, H. T.; Cheng, H. M.; Dresselhaus, M. S. *Science* 1999, 286, 1127.
- Baughman, R. H.; Cui, C.; Zakhidov, A. A.; Iqbal, Z.; Barisci, J. N.; Spinks, G. M.; Wallace, G. G.; Mazzoldi, A.; Rossi, D. D.; Rinzler, A. G.; Jaschinski, O.; Roth, S.; Kertesz, M. *Science* 1999, 284, 1340.
- De Heer, W. A.; Chatelain, A.; Ugarte, D. *Science* 1995, 270, 1179.
- Kong, J.; Franklin, N. R.; Zhou, C.; Chapline, M. G.; Peng, S.; Cho, K.; Dai, H. *Science* 2002, 287, 622.
- Tans, S. J.; Verschueren, A. R. M.; Dekker, C. *Nature* 1998, 393, 49.
- Bahr, J. R.; Yang, J.; Kosynkin, D. V.; Bronikowski, M. J.; Smalley, R. E.; Tour, J. M. *J Am Chem Soc* 2001, 123, 6536.
- Pompeo, F.; Resasco, D. E. *Nano Lett* 2002, 2, 369.
- Shafer, M. S. P.; Fan, X.; Windle, A. H. *Carbon* 1998, 36, 1603.
- Lee, H.-J.; Oh, S.-J.; Choi, J.-Y.; Kim, J. W.; Han, J.; Tan, L.-S.; Baek, J.-B. *Chem Mater* 2005, 17, 5057.
- Baek, J.-B.; Lyons, C. B.; Tan, L.-S. *Macromolecules* 2004, 37, 8278.
- Niyogi, S.; Hamon, M. A.; Hu, H.; Zhao, B.; Bhowmik, P.; Sen, R.; Itkis, M. E.; Haddon, R. C. *Acc Chem Res* 2002, 35, 1105.
- Bahr, J. L.; Tour, J. M. *J Mater Chem* 2002, 12, 1952.
- Baek, J.-B.; Tan, L. S. *Polymer* 2003, 44, 4135.
- Baek, J.-B.; Park, S.-Y.; Price, G. E.; Lyons, C. B.; Tan, L. S. *Polymer* 2005, 46, 1543.
- Hamon, M. A.; Hu, H.; Bhowmik, P.; Niyogi, S.; Zhao, B.; Itkis, M. E.; Haddon, R. C. *Chem Phys Lett* 2001, 347, 8.
- O'Connell, M. J.; Boul, P.; Ericson, L. M.; Huffman, C.; Wang, Y.; Haroz, E.; Kuper, C.; Tour, J.; Ausman, K. D.; Smalley, R. E. *Chem Phys Lett* 2001, 342, 265.
- Kong, J.; Dai, H. *J Phys Chem B* 2001, 105, 2890.
- Chen, Q.; Dai, L.; Gao, M.; Huang, S.; Mau, A. *J Phys Chem B* 2001, 105, 618.
- Kweona, H. Y.; Yoo, M. K.; Park, I. K.; Kim, T. H.; Lee, H. C.; Lee, H.-S.; Oh, J.-S.; Akaike, T.; Cho, C.-S. *Biomaterials* 2003, 24, 801.

23. Lim, K. Y.; Kim, B. C.; Yoon, K. J. *J Appl Polym Sci* 2003, 88, 131.
24. Gain, O.; Espuche, E.; Pollet, E.; Alexandre, M.; Dubois, Ph. *J Polym Sci Part B: Polym Phys* 2005, 43, 205.
25. <http://www.iljinnanotech.co.kr>.
26. Valentini, L.; Biagiotti, J.; López-Manchado, M. A.; Santucci, S.; Kenny, J. M. *Polym Eng Sci* 2004, 44, 303.
27. Liu, X.; Wu, Q. *Polymer* 2001, 42, 10013.
28. Woo, E. M.; Mandal, T. K.; Lee, S. C. *Colloid Polym Sci* 2000, 278, 1032.
29. Ma, J.; Zhang, S.; Qi, Z.; Li, G.; Hu, Y. *J Polym Sci* 1978 2002, 83.
30. Jin, Z.; Pramoda, K. P.; Xu, G.; Goh, S. H. *Chem Phys Lett* 2001, 337, 43.
31. Di, Y.; Iannace, S.; Maio, E. D.; Nicolais, L. *J Polym Sci Part B: Polym Phys* 2003, 41, 670.
32. Pötschke, P.; Abdel-Goad, M.; Alig, I.; Dudkin, S.; Lellinger, D. *Polymer* 2004, 45, 8863.
33. Liu, C.; Zhang, J.; He, J.; Hu, G. *Polymer* 2003, 44, 7529.